α-Fe 2O 3 hollow structures: Formation of single crystalline thin shells

ARTICLE *in* CHEMICAL COMMUNICATIONS · MAY 2012

Impact Factor: 6.83 · DOI: 10.1039/c2cc33032f · Source: PubMed

ChemComm

Cite this: *Chem. Commun.*, 2012, **48**, 6529–6531

www.rsc.org/chemcomm

COMMUNICATION

α-Fe_2O_3 hollow structures: formation of single crystalline thin shells†

Bing Xu,[a] Baibiao Huang,*[a] Hefeng Cheng,[a] Zeyan Wang,[a] Xiaoyan Qin,[a] Xiaoyang Zhang[a] and Ying Dai[b]

Received 5th March 2012, Accepted 11th May 2012
DOI: 10.1039/c2cc33032f

Novel α-Fe_2O_3 hollow polyhedra structures with single crystalline thin shells were synthesized by a facile one-pot template-free hydrothermal method, which exhibit high efficiency on the decoloration of RhB aqueous solution in the presence of H_2O_2. Based on experimental analysis, a plausible growth process is proposed.

The synthesis of inorganic nanomaterials with ordered morphologies and structures has received much interest because they have great influence on their physical/chemical properties.[1] In particular, hollow structures have been attracting increasing attention owing to their unique properties and widespread potential applications in many fields such as catalysis, magnetic materials, sensors, lithium storage and so on.[2] However, most reported hollow structures are hollow spheres whose shells are polycrystalline or made up of primary blocks. In contrast, the construction of nonspherical hollow nanocrystals with well-defined shapes is still a great challenge. Recently, due to their specific physical and chemical properties, hollow polyhedral structures have aroused intense interest.[3] For example, using shape-controlled Cu_2O crystals as sacrificial templates, Cu_xS nonspherical mesocages with single-crystalline shells could be well synthesized.[4] Nonetheless, these nonspherical hollow structures usually resorted to templates and the sacrificial-template route is not facile due to the following reasons. First, the nonspherical precursors are seldom found, second, uniform coating of the performed materials onto nonspherical precursors is difficult, finally, subsequent high-temperature calcination[5] or corrosion[6] process of precursors further complicate the synthetic procedure. Therefore, developing a facile one-pot template-free method to prepare nonspherical hollow structures becomes very significant.

In the past few years, several novel mechanisms including the Kirkendall effect, Ostwald ripening and self-assembled techniques have been developed to synthesize various hollow inorganic micro-/nanostructures.[7] However, the majority of the products obtained from these approaches are hollow spheres. Recently, zeolite analcime with core/shell or hollow icositetrahedra architectures were prepared by a one-pot hydrothermal route and the interesting growth mechanism of reversed crystal growth was proposed.[8] The processes of reversed crystal growth mainly include self-assembly of nanoparticles, surface recrystallization, and recrystallization from the surface to the core. Reversed crystal growth has great potential in the materials synthesis field, however, it has only been definitely confirmed in the fabrication of some zeolites,[9] titanate[10,11] and organic nanocrystals.[12] It is indispensable and crucial to expand the application of reversed crystal growth in the preparation of other inorganic materials.

As an n-type semiconductor, hematite (α-Fe_2O_3) is regarded as a promising material with potential applications in many fields owing to its high resistance to corrosion, low processing cost and nontoxicity. In order to explore its novel properties and expand its applications, many efforts have been devoted to the synthesis of α-Fe_2O_3 with various morphologies,[13] such as nanorings, nanowires, flower-like microspheres and hollow structures. Nevertheless, there are few reports on hematite with hollow polyhedra structures synthesized by a template-free route.

Herein, we develop a facile one-pot template-free hydrothermal method to prepare α-Fe_2O_3 hollow polyhedra. $FeCl_3 \cdot 6H_2O$ as iron source was dissolved in water and then C_4MimBF_4 (1-butyl-3-methylimidazolium tetrafluoroborate) which plays a key role in the formation of hollow polyhedra structures was added. After stirring for 3 h, the clear solution was transferred into a 100 ml Teflon-lined stainless steel autoclave, and maintained at 200 °C for 15 h. Fig. 1a shows a typical transmission electron microscopy (TEM) image of α-Fe_2O_3 hollow polyhedra and the size of the polyhedra ranges from 0.5 to 1 μm. It can be observed that the polyhedra have clear hollow interior voids with holes on their surfaces. The hollow polyhedra with smooth surfaces have 18 facets (Fig. S1, ESI†). According to the previous report, hematite octodecahedra polyhedra, which were not hollow structures,

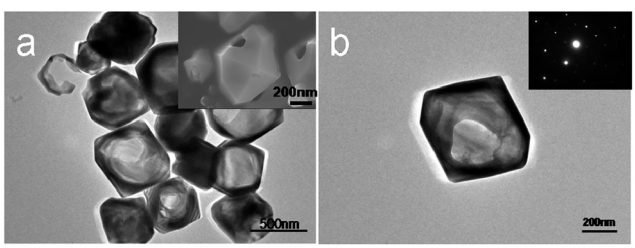

Fig. 1 TEM images (a, b) of α-Fe_2O_3 hollow polyhedra prepared at 200 °C for 15 h. Insets: (a) SEM image of single hollow polyhedron, (b) SAED pattern of single hollow polyhedron.

[a] *State Key Lab of Crystal Materials, Shandong University, Jinan 250100, People's Republic of China. E-mail: bbhuang@sdu.edu.cn*
[b] *School of Physics, Shandong University, People's Republic of China*
† Electronic supplementary information (ESI) available. See DOI: 10.1039/c2cc33032f

were enclosed by twelve (101) and six (111) planes.[14] The hollow polyhedra have the same planes as the hematite octodecahedra. Fig. 1b shows a single hollow polyhedron. The selected area electron diffraction (SAED) pattern corresponding to the single hollow polyhedron is shown as an inset in Fig. 1b, which demonstrates the single-crystalline nature of the hollow polyhedra.

To further investigate the formation mechanism of these novel α-Fe_2O_3 hollow structures, experiments were carried out at 200 °C for different reaction times to monitor the morphological evolution process of the nanoparticles. As shown in Fig. 2a, flower-like nanocrystals comprised of nanorods were obtained after hydrothermal synthesis for 2 h, which are demonstrated to be FeOOH by the corresponding XRD pattern (Fig. S2a, ESI†). When the reaction time was increased to 2.75 h, near-spherical solid particles and some debris were produced (Fig. 2b). According to the XRD pattern (Fig. S2b, ESI†) and the HRTEM images (Fig. S3, ESI†), nearly spherical solid particles with poor crystallinity and the debris can be identified as α-Fe_2O_3 and FeOOH, respectively. When the reaction time was increased further to 7 h, FeOOH debris disappeared and α-Fe_2O_3 polyhedra particles with imperfect surfaces with some pits were formed (Fig. 2c). According to the corresponding TEM images, the samples prepared with reaction times of 2.75 and 7 h are solid. When the reaction time reached 15 h, most polyhedra transformed to hollow structures, which usually had holes on their surfaces, though there are still some solid and core–shell structures (Fig. 2d). The samples which were prepared for 7 and 15 h are confirmed to α-Fe_2O_3 by the corresponding XRD patterns (Fig. S2c and d, ESI†).

In order to investigate the role of C_4MimBF_4 on the formation of the α-Fe_2O_3 hollow polyhedra structures, comparison experiments were also carried out without additive (Fig. S4a, ESI†) and with C_4MimCl (1-butyl-3-methylimidazolium chloride) (Fig. S4b, ESI†), $NaBF_4$ (Fig. S4c, ESI†) and NaF (Fig. S4d, ESI†) instead of C_4MimBF_4 as additives, while other experimental conditions were kept unchanged. According to the observations of Fig. S4 (see ESI†), we can come to the following conclusions. The F^- anions have an influence on the formation of polyhedra structures, but no influence on hollow structures. The presence of BF_4^- is key for the formation of hollow polyhedra structures because of its coordination with Fe^{3+}, while C_4Mim^+ simply contributes to improving the uniformity of the samples.

Based on the above analysis, a plausible formation mechanism of the α-Fe_2O_3 hollow polyhedra is proposed as represented in Scheme 1. In detail, there are essentially three reactions during the hydrothermal process as follows:

$$Fe^{3+} + 2H_2O \rightarrow FeOOH + 3H^+$$

$$2FeOOH \xrightarrow{\text{hydrothermal}} \alpha\text{-}Fe_2O_3 + H_2O$$

$$\alpha\text{-}Fe_2O_3 + 6H^+ \rightarrow 2Fe^{3+} + 3H_2O$$

First, Fe^{3+} ions react with water to form flower-like FeOOH particles at early stages with the formation of H^+ ions. Subsequently, the FeOOH particles are dehydrated to form α-Fe_2O_3 with poor crystallinity. These near-spherical α-Fe_2O_3 particles with low crystallinity were unstable under hydrothermal conditions due to their large surface energy. The surrounding acid solution and the large surface energy would contribute to the dissolution and recrystallization of the crystal facets. The rough surfaces recrystallized and became smooth, and transformed to a single crystalline thin shell. Meanwhile, the presence of BF_4^- ions, which absorbed on the surface of the particles, would be favorable on the formation of α-Fe_2O_3 octodecahedra. Then polyhedral structures with low crystallinity cores gradually formed with prolonged reaction times. In comparison with the single crystalline thin shell, the core is easily dissolved due to its poor crystallinity and higher surface energy. As the reaction proceeded, the core was gradually dissolved and core–shell structures were obtained. Fig. 2d clearly shows several particles with partially dissolved cores. When the core dissolved completely, hollow polyhedra structures were finally obtained.

Fig. 3a shows the UV-Vis diffuse reflectance spectra of α-Fe_2O_3 hollow polyhedra (15 h reaction time; S-15 h). The sample exhibits strong absorption in the visible range up to *ca.* 650 nm. To evaluate the photodegradation properties of as-prepared samples, photodegradation of rhodamine B (RhB) aqueous solution under visible light irradiation ($\lambda > 420$ nm) was carried out in the presence of H_2O_2. As shown in Fig. 3b, the self-degradation of RhB aqueous solution without the addition of catalysts or H_2O_2 is almost negligible, only about 10% of RhB molecules were degraded in 150 min. When H_2O_2 were added to the RhB aqueous solution, the degradation rate

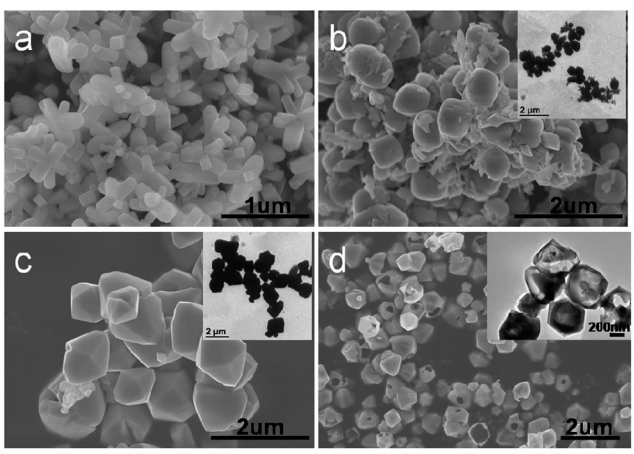

Fig. 2 SEM images of the samples synthesized for different reaction times under hydrothermal condition: (a) 2 h, (b) 2.75 h, (c) 7 h, (d) 15 h. Insets: the corresponding TEM images.

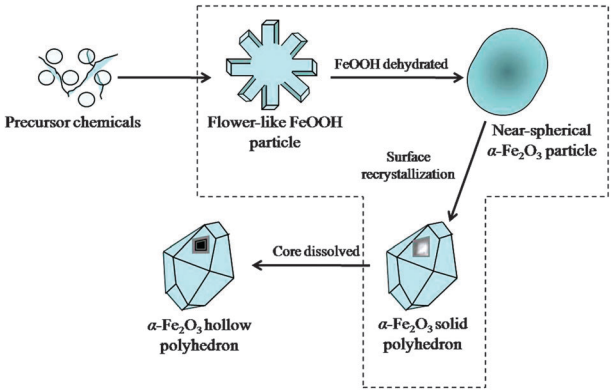

Scheme 1 Schematic illustration for the growth mechanism of α-Fe_2O_3 hollow polyhedra.

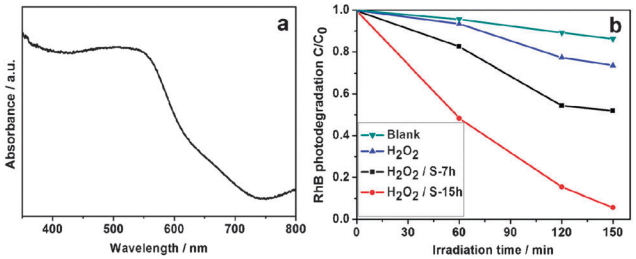

Fig. 3 (a) UV-Vis diffuse reflectance spectra of the S-15 h sample. (b) Photodegradation of RhB under visible light irradiation ($\lambda > 420$ nm). C and C_0 denote the reaction and initial concentration of RhB; S-7 h and S-15 h correspond to samples prepared at 200 °C for 7 and 15 h, respectively.

increased a little, which could be attributed to the presence of highly oxidative •OH formed by the photo-decomposition of H_2O_2. However, when α-Fe_2O_3 samples were added the photodegradation rates increased obviously which indicates the as-prepared α-Fe_2O_3 samples can promote the photodegradation of RhB in the presence of H_2O_2 under visible light irradiation (the photodegradation mechanism is discussed in ESI†). About 50% of RhB molecules were degraded for α-Fe_2O_3 solid polyhedra (S-7 h) after irradiation for 150 min while more than 90% RhB molecules were degraded for α-Fe_2O_3 hollow polyhedra (S-15 h) for the same irradiation time, which is due to the unique hollow structure. The BET specific surface area of α-Fe_2O_3 polyhedra and hollow polyhedra were measured to be 6.53 and 10.27 $m^2\ g^{-1}$, respectively. Compared to the solid polyhedra, the hollow polyhedra have higher specific surface area which can provide more reaction sites. In addition, the single crystalline thin shells decrease the migration distance of photogenerated carries from the interior to the surface. This results in decrease of recombination probability and so enhancement of photodegradation activity.

In summary, α-Fe_2O_3 hollow polyhedra have been prepared by a one-pot template-free hydrothermal method using C_4MimBF_4 as additive. The structures, morphologies and growth mechanism of the α-Fe_2O_3 hollow polyhedra were systematically investigated. Based on our experimental analysis, we find C_4MimBF_4 played an important role on the formation of hollow polyhedral structures with uniform size. In detail, BF_4^- is key for the formation of the hollow polyhedra structures because of its coordination with Fe^{3+}, while C_4Mim^+ contributes to improve the uniformity of the samples. A plausible growth process is proposed based on the experiment results, which mainly contains three stages including the formation of FeOOH, FeOOH dehydration to form α-Fe_2O_3 and surface recrystallization, and dissolution of the core. The growth mechanism is similar to the previously reported reversed crystal growth. The as-obtained α-Fe_2O_3 hollow polyhedra show a strong visible light absorption and exhibit high efficiency on the decolorization of RhB aqueous solution in the presence of H_2O_2. Considering the unique structure, the prepared α-Fe_2O_3 hollow polyhedra may find promising applications in other fields such as sensors, biomedical engineering and magnetics.

This work was financially supported by research grants from the National Natural Science Foundation of China (Nos. 20973102, 51021062, 51002091 and 21007031) and Natural Science Foundation of Shandong province (ZR2010BQ005).

Notes and references

1 J. B. Lian, X. C. Duan, J. M. Ma, P. Peng, T. Kim and W. J. Zheng, *ACS Nano*, 2009, **3**, 3749.
2 (*a*) J. X. Yu, B. B. Huang, Z. Y. Wang, X. Y. Qin, X. Y. Zhang and P. Wang, *Inorg. Chem.*, 2009, **48**, 10548; (*b*) H. F. Cheng, B. B. Huang, Z. Y. Wang, X. Y. Qin, X. Y. Zhang and Y. Dai, *Chem.–Eur. J.*, 2011, **17**, 8039; (*c*) Y. Wang, Q. S. Zhu and L. Tao, *CrystEngComm*, 2011, **13**, 4652; (*d*) Z. C. Wu, K. Yu, S. D. Zhang and Y. Xie, *J. Phys. Chem. C*, 2008, **112**, 11307; (*e*) J. Y. Zhong, C. B. Cao, Y. Y. Liu, Y. N. Li and W. S. Khan, *Chem. Commun.*, 2010, **46**, 3869; (*f*) Y. R. Ma and L. M. Qi, *J. Colloid Interface Sci.*, 2009, **335**, 1.
3 (*a*) X. W. Lou, C. L. Yuan, Q. Zhang and L. A. Archer, *Angew. Chem., Int. Ed.*, 2006, **45**, 3825; (*b*) J. H. Yang, L. M. Qi, C. H. Lu, J. M. Ma and H. M. Cheng, *Angew. Chem., Int. Ed.*, 2005, **44**, 598; (*c*) Z. Y. Wang, D. Y. Luan, C. M. Li, F. B. Su, S. Madhavi, F. Y. C. Boey and X. W. Lou, *J. Am. Chem. Soc.*, 2010, **132**, 16271; (*d*) C. H. Lu, L. M. Qi, J. H. Yang, X. Y. Wang, D. Y. Zhang, J. L. Xie and J. M. Ma, *Adv. Mater.*, 2005, **17**, 2562.
4 S. H. Jiao, L. F. Xu, K. Jiang and D. S. Xu, *Adv. Mater.*, 2006, **18**, 1174.
5 J. G. Yu, X. X. Yu, B. B. Huang, X. Y. Zhang and Y. Dai, *Cryst. Growth Des.*, 2009, **9**, 1474.
6 Y. Wang, X. W. Su and S. Lu, *J. Mater. Chem.*, 2012, **22**, 1969.
7 (*a*) B. Liu and H. C. Zeng, *J. Am. Chem. Soc.*, 2004, **126**, 16744; (*b*) X. W. Lou, Y. Wang, C. L. Yuan, J. Y. Lee and L. A. Archer, *Adv. Mater.*, 2006, **18**, 2325; (*c*) H. G. Yu, J. G. Yu, S. W. Liu and S. Mann, *Chem. Mater.*, 2007, **19**, 4327; (*d*) F. Caruso, *Chem.–Eur. J.*, 2000, **6**, 413; (*e*) A. M. Cao, J. S. Hu, H. P. Liang and L. J. Wan, *Angew. Chem., Int. Ed.*, 2005, **44**, 4391; (*f*) X. W. Lou, L. A. Archer and Z. C. Yang, *Adv. Mater.*, 2008, **20**, 3987; (*g*) Q. Zhang, W. S. Wang, J. Goebl and Y. D. Yin, *Nano Today*, 2009, **4**, 494.
8 X. Y. Chen, M. H. Qiao, S. H. Xie, K. N. Fan, W. Z. Zhou and H. Y. He, *J. Am. Chem. Soc.*, 2007, **129**, 13305.
9 W. Z. Zhou, *Adv. Mater.*, 2010, **22**, 3086.
10 X. F. Yang, J. X. Fu, C. J. Jin, J. Chen, C. L. Liang, M. M. Wu and W. Z. Zhou, *J. Am. Chem. Soc.*, 2010, **132**, 14279.
11 H. Q. Zhan, X. F. Yang, C. M. Wang, J. Chen, Y. P. Wen, C. L. Liang, H. F. Greer, M. M. Wu and W. Z. Zhou, *Cryst. Growth Des.*, 2012, **12**, 1247.
12 J. R. G. Sander, D. K. Bucar, J. Baltrusaitis and L. R. MacGillivray, *J. Am. Chem. Soc.*, 2012, **134**, 6900.
13 (*a*) X. L. Hu, J. C. Yu, J. M. Gong, Q. Li and G. S. Li, *Adv. Mater.*, 2007, **19**, 2324; (*b*) F. Meng, S. A. Morin and S. Jin, *J. Am. Chem. Soc.*, 2011, **133**, 8408; (*c*) L. S. Zhong, J. S. Hu, H. P. Liang, A. M. Cao, W. G. Song and L. J. Wan, *Adv. Mater.*, 2006, **18**, 2426; (*d*) Z. Y. Wang, D. Y. Luan, C. M. Li, F. B. Su, S. Madhavi, F. Y. C. Boey and X. W. Lou, *J. Am. Chem. Soc.*, 2010, **132**, 16271; (*e*) L. L. Li, Y. Chu, Y. Liu and L. H. Dong, *J. Phys. Chem. C*, 2007, **111**, 2123; (*f*) S. Y. Zeng, K. B. Tang, T. W. Li, Z. H. Liang, D. Wang, Y. K. Wang and W. W. Zhou, *J. Phys. Chem. C*, 2007, **111**, 10217.
14 B. L. Lv, Z. Y. Liu, H. Tian, Y. Xu, D. Wu and Y. H. Sun, *Adv. Funct. Mater.*, 2010, **20**, 3987.